International Journal of ISSI, Vol.5 (2008), No. 1, pp. 15-21

Factors Affecting Weldability Improvement of Dissimilar Welds of Aged HP Stainless Steel and Alloy 800

R. Dehmolaei[1], M. Shamanian[2*] and A. Kermanpur[3]
Department of Materials Engineering, Isfahan University of Technology, Isfahan 84156-83111, Iran
Received December 31, 2007; Accepted February 26, 2008

Abstract
The microstructure of HP stainless steel in aged and aged + solution annealed conditions and solutionized alloy 800 was characterized by optical microscopy, scanning electron microscopy (SEM), and transmission electron microscopy (TEM) equipped by EDS. All phases present in the above condition were described. The effects of solution annealing heat treatment temperature on the microstructure, tensile, hardness, toughness, and ductility of aged HP stainless steel and its weldability to alloy 800 have been discussed. In addition, the effects of heat input, interpass temperature, and type of filler metal on weldability of two alloys were investigated. It was found that during solution annealing, the precipitates produced in the aging stage are decomposed and niobium carbide (NbC) is formed. It was also observed that while tensile strength and hardness fell, ductility and toughness were improved. Dissimilar welding between alloy 800 and aged HP stainless steel was not successful and cracks were observed in the HAZ of the aged HP stainless steel, while welding alloy 800 to HP stainless steel (aged + solution annealing at 1100-1200°C, low interpass temperature, and Inconel 82 or 617 filler metals) was successful.

Keywords: Dissimilar welding, Weldability, Solution annealing, HP steel, Alloy 800.

1- Introduction

Cast heat-resistant steels are used in applications where service temperature exceeds 650°C. These steels have superior creep strength, resistance to corrosion at elevated temperatures, and stability (resistance to warping, cracking, or thermal fatigue) [1]. HP stainless steel (35%Ni-25%Cr) is a heat-resistant steel that has a combination of creep strength and resistance to oxidizing and carburizing atmospheres at high temperatures [1]. This alloy has been recently used to fabricate petrochemical and refinery components which are employed at such high temperatures as steam gas reformer tubes and cracking tube materials of naphtha [3-5]. HP stainless steel is usually used under the cast condition with an austenitic matrix containing continuous chains of primary eutectic carbides, and is not susceptible to σ-phase formation [1,2,5]. In addition, secondary carbides and intermetallic compounds are precipitated within the austenitic matrix and grain boundaries upon exposure to elevated temperatures [1-3, 6]. The precipitation of carbides and the formation of intermetallic compounds are responsible for the strengthening and the loss of ductility at temperatures of about 500-750°C [1,2,6]. The strength is reduced after long-term exposure to higher temperatures (900-1200°C), while ductility is improved [1, 6-9].

Weld repair of oil refinery components has become increasingly prevalent for prolonging component life and for reducing the costs associated with component replacement. Therefore, repair of dissimilar welds between HP stainless steel and other alloys (such as alloy 800) is necessary in many high-temperature applications. The gas reformer tubes and headers of Isfahan Oil Refinery are made of HP stainless steel and alloy 800, respectively. Joints are needed of these alloys for repairs and replacement of worn-out workpieces (under long-term service). Heat affected zone (HAZ) cracking is the main weldability problem in repairing these alloys [9].

In this work, a solution heat treatment is proposed to overcome the problem. The effects of solution annealing temperature of aged HP stainless steel on its microstructure, mechanical properties, and weldability to alloy 800 are investigated. In addition, the effects of heat input, interpass temperature, and type of filler metal on the weldability are studied.

2- Materials and Methods

The aged HP stainless steel (at 820°C for 1500h) and alloy 800 base metals were used in tube shape for the purposes of the present study. The tubes

*Corresponding author:
Tel:+98- 311-3915737 Fax:+98- 311-3915737
E-mail: shamanian@cc.iut.ac.ir
Address: Dept. of Materials Engineering,
Isfahan University of Technology, Isfahan 84156-83111, Iran

1. PhD Candidate
2. Associate Professor
3. Assistant Professor

were 13.5 mm thick and the external diameters of HP stainless steel and alloy 800 were 250 and 320mm, respectively. The chemical compositions of the base and the filler metals used were as presented in Table 1. Several coupons with 100×100×13mm dimensions were prepared from the tubes. A number of the coupons prepared from the aged HP stainless steels were subjected to a solution annealing heat treatment for 2h at 1000, 1100, and 1200°C in an electric box furnace. Two alloys were welded together using gas tungsten arc welding using the direct current electrode negative (GTAW-DCEN) process. Two types of joints, namely, aged HP stainless steel/solutionized alloy 800 and HP stainless steel (aged + solution annealing)/solutionized alloy 800 were produced. The welds were produced using four heat inputs (710, 820, 935, and 1150 J/mm), four interpass temperatures (continuous welding, 500, 200, and 25°C), and four types of filler metal (Inconel 82, 182, 617, and 309 stainless steel). The joints were prepared by machining to 75° groove angles. The welding parameters are shown in Table 2. The gas protection used was 99% pure argon (25 and 40 CFH, flow rate for backing and shielding). For metallographic examinations, specimens 10×20×40 mm in size were cut from the base metals and weldments. All specimens were ground on silicon carbide paper of 80-2000 grit, and polished on a nylon cloth with 0.3μm alumina paste. The etching reagent used for revealing the microstructure was marbel (10 gr $CuSO_4$ + 50cc HCl + 50cc H_2O). The microstructures were identified using optical microscopy and scanning electron microscopy (SEM) equipped with energy dispersive spectroscopy (EDS) point analysis. Tensile and impact samples of base metals under different conditions were prepared and subjected to similar treatments to evaluate variations of mechanical properties. Tensile tests were carried out for the base metals according to ASTM E8 Standard. Charpy V-notch impact tests were carried out for the base metals according to ASTM E23 M Standard and room temperature toughness of the base metals were measured. Tensile and impact tests of the weld metals were performed according to AWS B4 Standard. Hardness of all samples was measured by Vickers method with 30N load.

Table 1. Chemical composition of the base and filler metals.

	Fe	Ni	Cr	C	Nb	Ti	Al	Mo	Mn	Si
HP steel	35.4	35.8	24.4	0.4	1.3	----	----	0.04	1.3	1.3
Alloy 800	39.5	31.1	17.9	0.09	----	0.36	0.25	----	1	0.7
Inconel 82	3	67	18.2	0.1	2-3	0.75	0.3	----	2.5	0.5

Table 2. Welding parameters.

	Root pass	Fill and cap passes
Current (A)	105	120
Voltage (V)	14	14
Travel speed (mms^{-1})	1.4	1.1
Heat input ($kJmm^{-1}$)	0.791	1.07

3- Results and discussion

3-1- Microstructures

Figure 1a shows the microstructure of the as-received alloy 800 to contain an austenitic matrix with precipitations in the matrix and along the grain boundaries. The image taken by SEM using backscattered electron (BSE) reveals two types of precipitates with different sizes and morphologies Figure 1b. The (coarser) cubic type lies in the matrix and on the grain boundaries, while the (finer) spherical type lies essentially within the matrix. Investigations showed that the cubic type is titanium nitride (or carbonitride) and the spherical one is titanium carbide (TiC) [6-10].

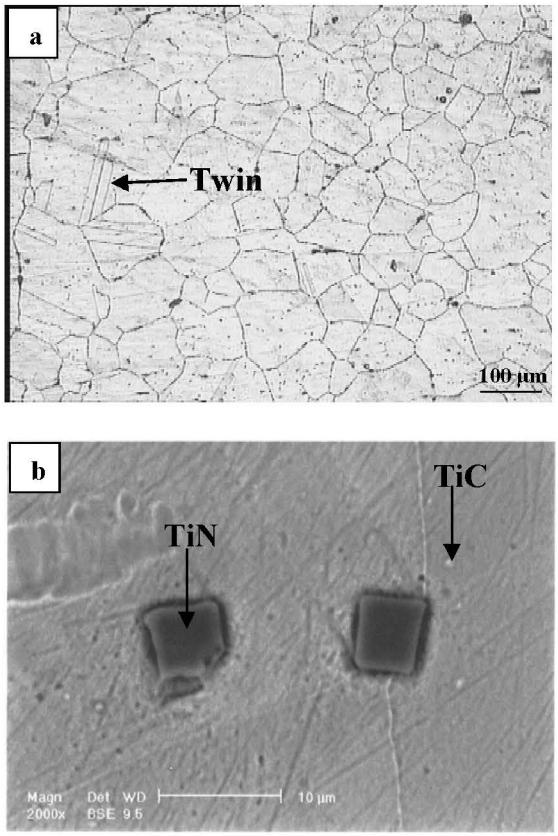

Fig. 1. Micrographs of alloy 800. (a) Light soptical micrograph; (b) SEM image using backscattered electrons.

The microstructure of the aged HP stainless steel base metal is shown in Figure 2. Optical micrograph Figure 2a shows a network of eutectic carbides with precipitates in the austenitic matrix and on the grain boundaries. The formation of these precipitates is due to metallurgical changes during aging at 820°C. In the micrograph obtained by SEM using BSE, three types of precipitates are observed Figure 2b: The first one which is fine and dark lies in the austenitic matrix while the second and third, one being dark and the other white, lie on the grain boundary. The EDS spectra obtained for these precipitates Figure 3

indicate that both the dark precipitates are rich in chromium and iron, while the white precipitates are rich in nickel, niobium, and silicon. These precipitates may be identified as M23C6 (M represents chromium and a small amount of iron) and G phase (Ni_{16} Nb_6 Si_7), respectively. The formation of these precipitates and other metallurgical changes (such as G phase transformation) can cause an increase in strength and a loss of ductility [6, 11-13]. A TEM micrograph of the aged HP stainless steel and EDS spectra of its precipitates are shown in Figure 4. Therefore, formation of the G phase has been confirmed by TEM. Many references have already reported presence of the G phase under the aged condition of HP steel [2, 14-17].

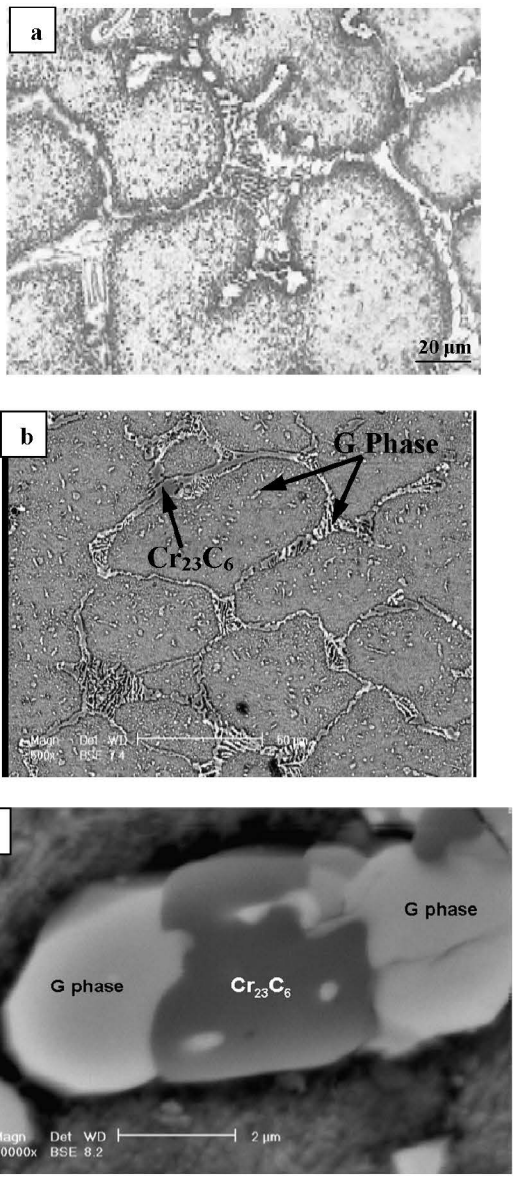

Fig. 2. Micrographs of aged HP steel. (a) Light optical micrograph; (b) SEM image with BSE; (c) SEM image of G phase.

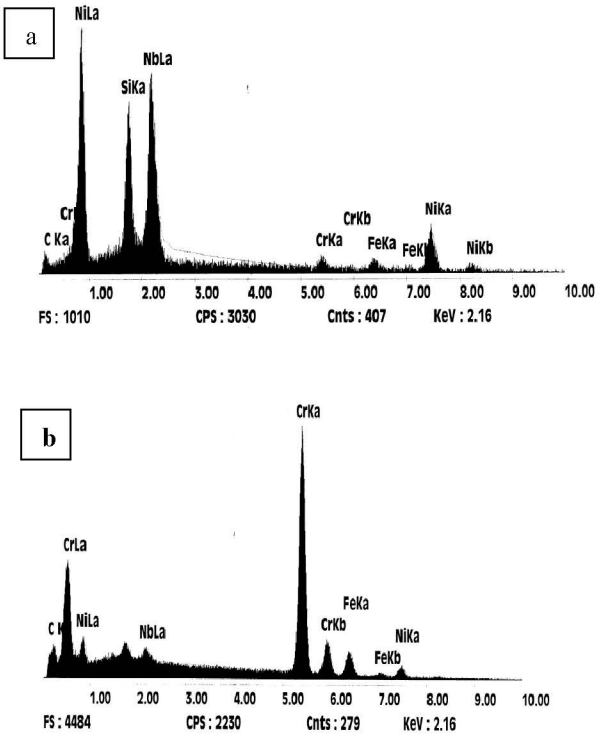

Fig. 3. EDS spectra of precipitates in the aged HP steel base metal. (a) white precipitates; (b) Dark precipitates.

Figure 5 shows the microstructures of aged HP stainless steel after solution annealing at different temperatures. The microstructure after solution annealing at 1000°C consists of eutectic carbides and a great number of undissolved secondary precipitates Figure 5a. Figure 5b shows that after solution annealing at 1100°C, a great amount of secondary precipitates is dissolved. Solution annealing at 1200°C causes the dissolution of secondary precipitates, plus even small amounts of primary eutectic carbides, and the recovery of the primary microstructure Figure 5c. Solution annealing at 1100-1200°C causes the dissolution of the G phase and Cr carbide ($Cr_{23}C_6$), because Cr carbide forms at a temperature range of about 650-850°C and dissolves at a higher temperature [18, 19]. The niobium carbide (NbC) is a high-temperature carbide that is formed at a temperature between 1100 and 1250°C over the shortest time [18]. Thus, at a temperature near 1200°C, the segregated niobium from the G phase has an extensive tendency to react with carbon. On the other hand, carbon diffuses from the austenitic matrix toward niobium to form niobium carbide (NbC) in the grain boundaries. More investigations by SEM confirmed the dissolution of carbide and the G phase at 1100-1200°C Figure 5d. Reformation of the niobium carbide was confirmed by EDS analysis Figure 6.

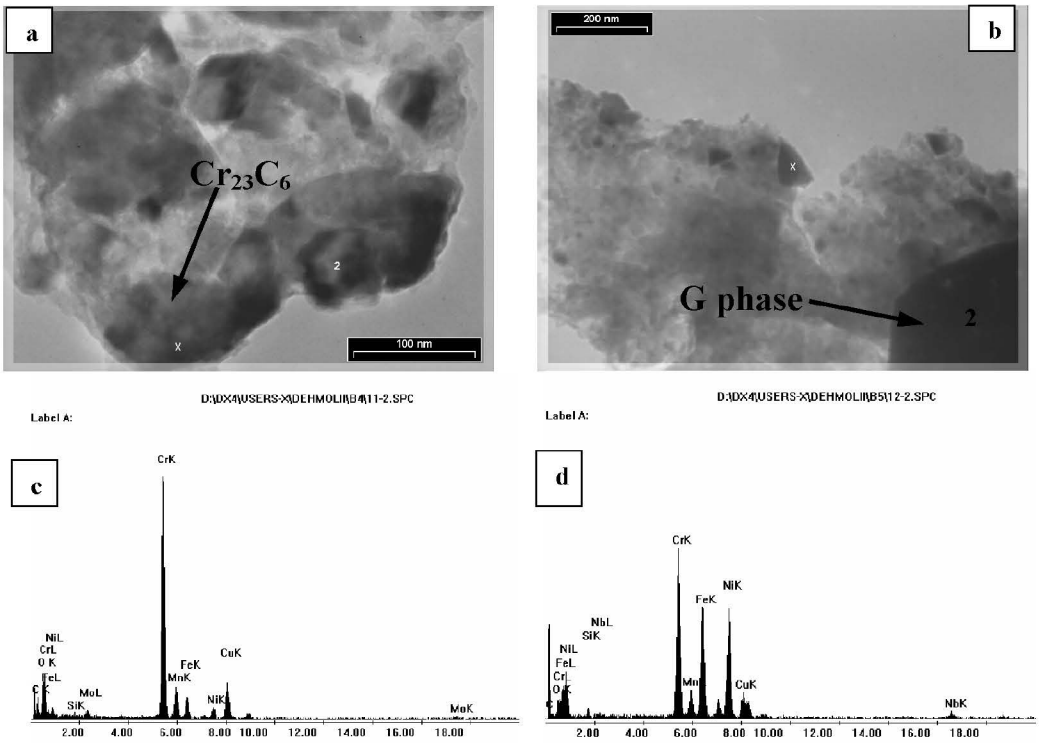

Fig. 4. (a) and (b) TEM micrographs of aged HP steel, showing details of the chromium carbide and G phase precipitates. (c) EDS spectrum for Chromium carbide, : (d) EDS spectrum for G-phase.

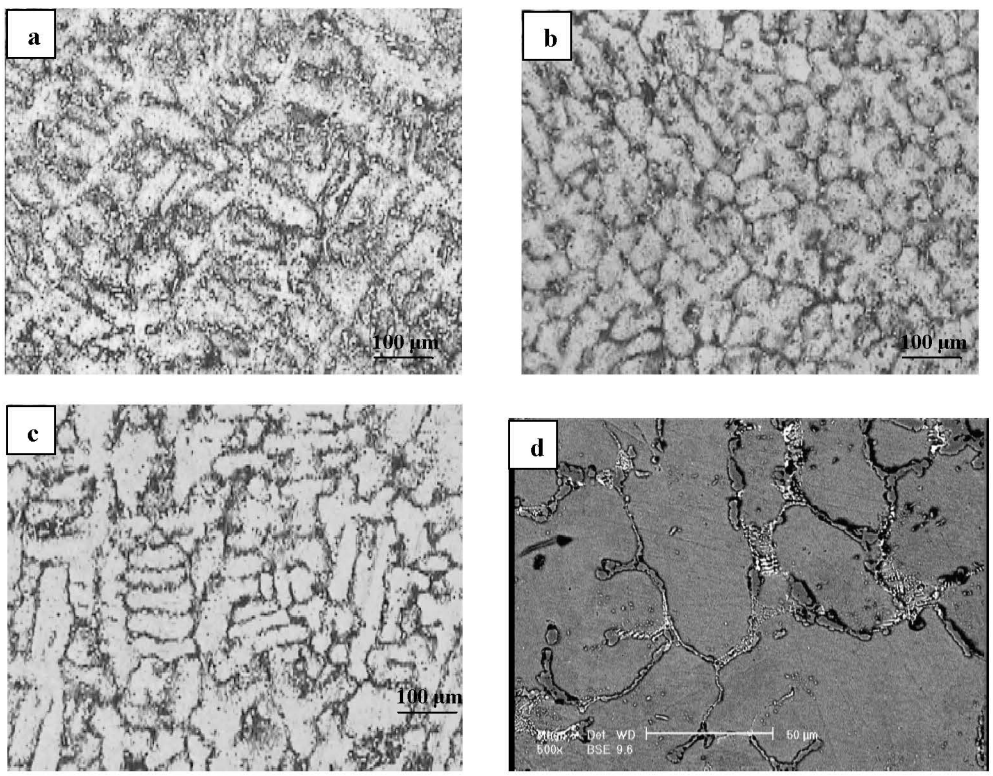

Fig. 5. Microstructure of the aged HP steel after solution annealing treatment for 2h at 1000 ℃, (b) 1100 ℃, (c) 1200 ℃, and (d) 1200 ℃ with SEM using BSE.

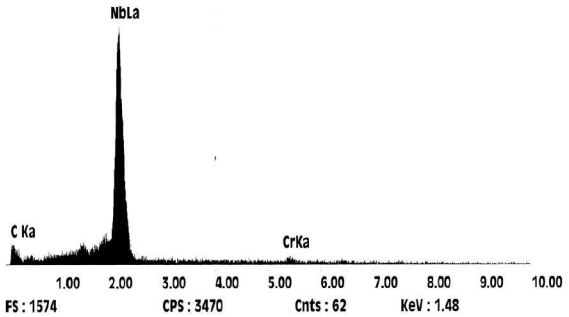

Fig. 6. EDS spectrum of the white precipitates in the aged HP steel after solution annealing heat treatment at 1200 ℃.

3-2- Mechanical Properties

Table 3 shows mechanical properties of the base metals under different conditions before welding. It is seen that the ductility of aged HP steel is about 3% (very low). This parameter is very important in welding since the material must be able to undergo plastic deformation during the heating and cooling cycles resulting from different passes of the welding. Table 3 shows that solution annealing decreases the strength and hardness of aged HP stainless steel, but increases its ductility and toughness. Also, it is seen that ductility and toughness extensively increase with increasing treatment temperature. Solution annealed at the temperature range of 1100-1200°C causes the dissolution of the carbides formed during aging (secondary carbides), some of the primary eutectic carbides ($M_{23}C_6$), and the G phase. This increases ductility and toughness but decreases strength and hardness.

3-3- Weldability

The interfaces between the weld and the base metals under various conditions are shown in Figures 7 to 9. All images indicate that the microstructure of the weld metal is finer than that of the base metal. The weld fusion line between the weld and as-received alloy 800 metals Figure 7a shows a continuous fusion trend. This figure shows that grain growth and grain boundary thickening take place in the HAZ of alloy 800 near the weld fusion line. Grain growth is caused by increasing the temperature of HAZ during the different passes of welding. Figure 7b shows that a crack is formed in the HAZ of aged HP stainless steel. It is observed that the cracks are of an intergranular type initiating from the grain boundary and growing through primary eutectic carbides. In this condition, the crack formation can be attributed to the loss of ductility and toughness (great embrittlement) and to the microstructural changes during aging. The formation of cracks during welding decreases weldability of the aged HP stainless steel. Therefore, dissimilar welding between aged HP stainless steel and alloy 800 is not possible. SEM micrographs using SE and BSE Figure7c and 7d confirm the presence of cracks and apparently show that they are of the intergranular type. In order to overcome this problem and to improve the weldability, four factors were contemplated: solution annealing heat treatment, selection of an appropriate filler metal, and changes in the heat input and interpass temperature. Investigations showed that the best results could be obtained with Inconel 82 and 617 filler metals, low heat input (820 to 710 J/mm), low interpass temperature (below 200°C), and solution annealing at 1100-1200°C. Figure 8 shows that cracking in the aged HP stainless steel/alloy 800 occurs at different levels of heat input and low interpass temperatures. The decrease in heat input and interpass temperature can improve the cracking resistance of aged HP stainless steel during welding, but it is not fully eradicated.

Table 3. Mechanical properties of HP steel base metal at different conditions.

	Yield strength (MPa)	Tensile strength (MPa)	Toughness (J)	Elongation (%)	Hardness (VHN)
HP steel	341	561	8.56	14.4	141
Aged HP steel	476.6	629.3	3.07	3	154
Heat treated HP steel at 1000°C	425	607.5	4.6	7.35	135
Heat treated HP steel at 1100°C	394.66	590.6	6.86	10.76	130
Heat treated HP steel at 1200°C	369	563	6.85	9.72	114

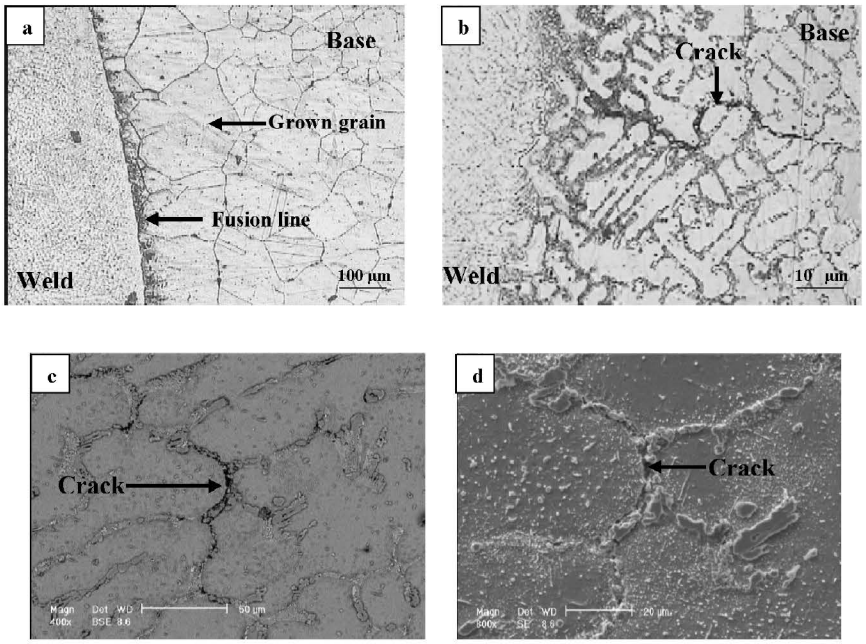

Fig. 7. Interfaces between the base metals and the weld metal. (a) Solutionized alloy 800; (b) Aged HP steel; (c) SEM image using BSE of crack in the HAZ of aged HP steel; (d) SEM image using SE of crack in the HAZ of aged HP steel.

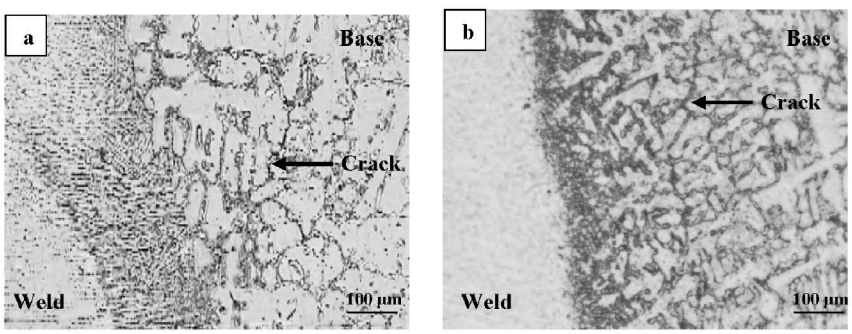

Fig. 8. Interfaces between the weld metal and aged HP steel base metal in different heat inputs: (a) 820 J and (b) 710 J.

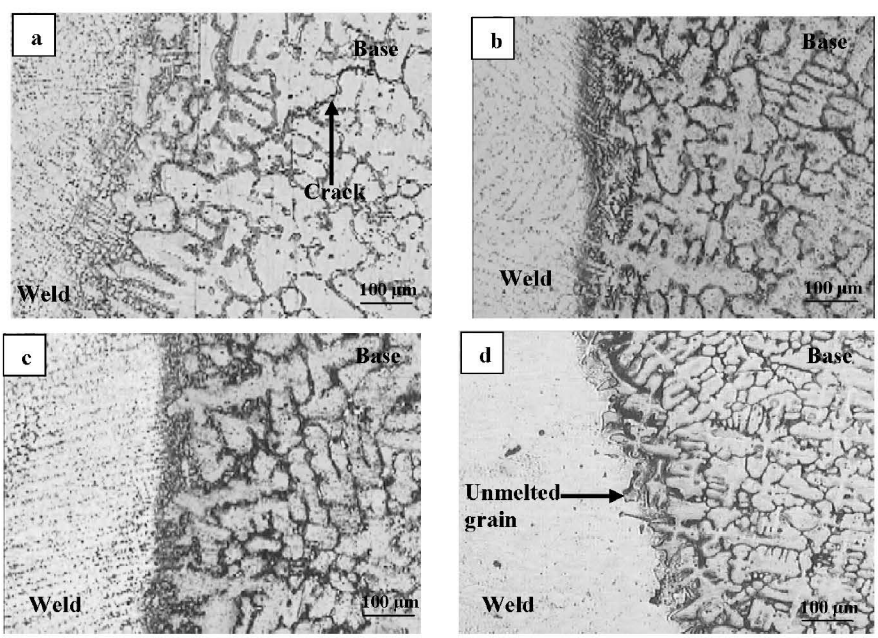

Fig. 9. Interfaces between the weld metal and aged HP steel base metal after solution annealing for 2h at (a) 1000 ℃, (b) 1100 ℃, (c) 1200 ℃, and (d) 1200 ℃ with Inconel 617 filler metal.

The interfaces between the solution annealed HP stainless steel base metal and weld metal (Inconel82 and 617 filler metals) are seen in Figure 9. Figure 9a shows that after solution-annealing at 1000°C, a crack is still present in the HAZ of HP stainless steel since many precipitates remain in this case while ductility has not yet improved very much. From the micrographs in Figures 9b and 9c, it is evident that cracks are eliminated after solution annealing at 1100 & 1200°C, thus improving weldability to a great extent. The increase in weldability in this case can be attributed to the increased ductility and toughness (See Table 3). An appropriate continuity can be observed between the weld and the base metals. Figure 9d shows that the Inconel 617 is a good filler metal and its interface with the base metals is continuous without any cracks. The results indicate that the solution annealing heat treatment is the most important step in the dissimilar weld repair of aged HP stainless steel to alloy 800.

4- Conclusions

- The microstructure of aged HP stainless steel consists of an austenitic matrix with primary carbides prior to aging. During aging, however, secondary carbides and the G phase ($Ni_{23}Nb_6Si_7$) are formed.
- During solution annealing (especially at 1100-1200°C), ductility and toughness are enhanced while the strength and hardness decrease.
- Dissolution of the secondary carbides and even some of the primary carbides, the G phase, and the reformation of niobium carbides (NbC) are the microstructural variations taking place during solution annealing of aged HP steel.
- It is observed that dissimilar welds of aged HP steel to solutionized alloy 800 lead to serious problems, and that intergranular cracking takes place in the HAZ of the HP steel during welding.
- Dissimilar welds between solution annealed HP steel and alloy 800 are satisfactory when solution annealing at 1100-1200°C, low heat input (710-820 J), interpass temperatures below 200°C and Inconel 82 or 617 filler metals are used.

References

[1] M. Blair and T. L. Stevens, Steel Casting Handbook, ASM International, (2000), 22.1.
[2] L. H. Almeida, A. F. Ribeiro, and I. Le May, Mater. Charact., 49(2003), 219.
[3] N. Kazutoshi, S. Kazuyoshi, I. Masahiro, and T. Makoto, Weld. Res. Abroad, 46(2000), 32.
[4] K. Shinozaki, K. Kuroki, K. Nishimoto, M. Lnuia and M. Takahashi, Weld. Res. Abroad, 45(1999), 22.
[5] R. Dehmolaei, M. Shamanian and A. Kermanpur, 59(2008), 1447.
[6] S. Haro, D. Lopez, A. Velasco and R. Viramontes, Mater. Chem. Phys., 66(2000), 90.
[7] M. Qian and J. C. Lippold, Mater. Sci. Eng. A, 340(2003), 225.
[8] T. Lant, D. L. Robinson, B. Spafford, and J. Storesund, Inter. J. Pres. Ves. Pip. 78(2001) , 813.
[9] M. Qian and J. C. Lippold, Acta Mater., 51(2003), 3351.
[10] M. Sireesha, V. Shankar, S. K. Albert and S. Sundaresan, Mater. Sci. Eng. A., 292(2000), 74.
[11] H. Sergio, C. Rafael, V. Abraham and L. David, Mater. Chem. Phys., 77(2002), 831.
[12] H. W. Ebert, Weld. J., (1976), 939.
[13] R. E. Avery, Weld. J., (1988), 43.
[14] F. C. Nunes, L. H. de Almeida, J Dille, J. L. Delplancke and I. Le May, Mater. Charact., 58(2007),132.
[15] R. A. Pedro Ibanez, G. D. de Almeidao, L. H. de Almeida and I. L. May, Mater. Charact., 30(1993), 243.
[16] R. A. Pedro Ibanez, T. L. da Silveria, L. H. de Almeida and I. L. May, Mater. Charact., 29(1992), 387.
[17] R. A. Pedro Ibanez, T. L. da Silveria, L. H. de Almeida and I. L. May, Mater. Charact., 26(1991), 193.
[18] S. Kou, Welding Metallurgy, John Wiley & Sons, Inc., New Jersey, (2003), 435.
[19] J. C. Lippold and D. J. Koteki, Welding Metallurgy and Weldability of Stainless Steels, John Wiley & Sons, Inc , New Jersey, (2005), 151.